Innovative 3D-Printed Titanium Specimens Favor a Modulation of Inflammation in Dental Pulp Stem Cells During Liposome-Triggered Mineralization

Marialucia Gallorini, PhD[1]/Alessia Ricci, PhD[1]/Serena Pilato, PhD[1,2]/Antonella Fontana, Prof[1,2]/
Carlo Mangano, MD[3]/Amelia Cataldi, Prof[1,2]/Susi Zara, Prof[1]

Purpose: To investigate the interplay between inflammation and differentiation upon implantation, dental pulp stem cells (DPSCs) were cultured on 3D-printed titanium owning an internal open cell form, administering osteogenic factors by a liposomal formulation (LipoMix) compared to traditional delivery of differentiation medium (DM). ***Materials and Methods:*** Osteogenic differentiation was evaluated via western blot by measuring β1 integrin expression and real-time reverse transcription-polymerase chain reaction (RT-PCR), as well as measuring SP7 and type 1 collagen gene expression. In addition, angiogenesis was characterized by measuring vascular endothelial growth factor (VEGF) secretion levels. Matrix mineralization was assessed by means of Alizarin red staining, cell adhesion, and inflammation responses through western blot, enzymatic, and enzyme-linked immunosorbent assays (ELISA) that evaluated Nrf2 expression, catalase activity, and prostaglandin E2 (PGE2) secretion, respectively. ***Results:*** LipoMix enhances cell proliferation and adhesion, as revealed by increased β1 integrin expression. Mineralized matrix deposition, SP7 gene expression, type 1 collagen release, and alkaline phosphatase activity appeared to increase in the LipoMix condition. Additionally, the redox-sensitive transcription factor Nrf2 was overexpressed at the earliest experimental times, triggering the catalase activity. ***Conclusions:*** The data reported confirmed that internal topography and post-production treatments on Ti surfaces dynamically and positively conditioned the DPSC progress toward the osteogenic phenotype; moreover, the combination with LipoMix quickened the positive modulation of inflammation under osteogenic conditions. Therefore, the development of customized surfaces along with the administration of differentiating factors enclosed in a liposomal delivery system could represent a promising and innovative tool in regenerative dentistry. *Int J Oral Maxillofac Implants 2025;40:427–438. doi: 10.11607/jomi.11129*

Keywords: osteogenic differentiation, NF-E2-related factor 2, liposomal formulation, stem cells, regenerative dentistry

Titanium (Ti) is a common material used in dentistry for the manufacturing of dental implants, crowns, and bridges. Thanks to its favorable characteristics, such as high corrosion resistance, good mechanical properties, biocompatibility with the surrounding tissues,[1,2] Ti is one of the most long-lasting materials used.[3] Osseointegration and postcondition, which are related to the cells' capability to anchor on the implant and to the bones' ability to grow on a specific surface,[4] are two of the main aspects of an efficient implant system. It has been widely demonstrated that Ti plays a pivotal role in this field, enticing osteoblasts and bone deposition and leading to the filling of the whole space between the implant and the surrounding tissue. Researchers are continuously focused on the optimization of Ti-based implant surfaces and internal topography characteristics by using different techniques, such as additive manufacturing, aiming at developing customized alloys with specific porosity and controlled surface features. In particular, it has been recently demonstrated that macro-porous Ti-based implants with an open interconnected structure, characterized by pores ranging from 200 to 400 µm, are able to guarantee a stable bone tissue placement that helps promote bone regeneration.[5,6]

In a previous study,[7] a laser-melted 3D-printed Ti-specimen (Ti A) was drawn in computer-aided-design (CAD) and produced via a laser melting technique with an open cell form. This was validated in terms of biocompatibility and capability to induce in vitro osteogenic differentiation. In accordance with the above reported results, the open cell inner form of Ti A, resembling the trabecular structure of bone tissue, demonstrated a faster osteogenic differentiation along with an

[1]Department of Pharmacy, University of Gabriele d'Annunzio, Cheiti-Pescara, Chieti, Italy.
[2]UdA Tech Lab, University of Gabriele d'Annunzio, Cheiti-Pescara, Chieti, Italy.
[3]Department of Dental Sciences, University San Raffaele, Milan, Italy.

Correspondence to: Prof Susi Zara, susi.zara@unich.it

Submitted July 10, 2024; accepted October 10, 2024.

Table 1 Description of Titanium Specimens

Material	Size/shape	Synthesis	Heat treatment	Post-production treatment
Ti_6Al_4V	Discs 5 mm in diameter and 2 in mm depth / Open cell form	• RenAM 500Q (Renishaw) • Laser power: 200 W • Speed: 0.9 m/s • Layer thickness: 15 µm	Vacuum heat treatment at 800°C for 1 hour	• Sonication for 5 minutes in deionized water at 25°C • Submersion in NaOH (20 g/L) and hydrogen peroxide (20 g/L) at 80°C for 30 minutes • Sonication for 5 minutes in deionized water • Submersion in a mixture of organic acids (50% maleic/oxalic) at 80°C for 45 minutes

ameliorated cell interaction with the scaffold surface, thus revealing a better bioactivity profile compared to standard Ti specimens.[7]

Immediately after placement, an inflammatory response is activated by the immune system and afterwards by cells of soft tissues, thus requiring a tight equilibrium between pro-inflammatory and anti-inflammatory processes to avoid implant rejection events.[8] Indeed, a dysregulated inflammatory condition affects the healthy tissue surrounding the implant and prevents osteomodulation,[9] however, an ineffective inflammatory response might interfere with material integration, osteogenic differentiation, and new tissue growth. Debris or particles released from the host implanted material or surgical trauma triggered by placement procedures require a balanced interaction between biomaterials and the immune response to obtain an optimal material inclusion.[10,11] Moreover, it has been also demonstrated that the intensity of the inflammatory response is related to surface characteristics and internal topography of Ti specimens, in particular hydrophilic and wettable rough Ti alloys appear to generate an anti-inflammatory microenvironment.[12]

Nuclear factor E2-related factor 2 (Nrf2) is a transcription factor regulating oxidative stress and attenuating inflammation through the translocation from the cytoplasmic compartment to the nuclear compartment, where it transcriptionally activates the following antioxidant enzyme genes: heme oxygenase-1, superoxide dismutase (SOD), glutathione peroxidase enzyme (GPX), and more.[13,14] Upon periodontitis, Nrf2 plays an important role in anti-apoptotic pathways, by reducing intracellular reactive oxygen species (ROS), inducing the transcription of anti-apoptotic and anti-inflammatory factors, or by contrasting the production of pro-inflammatory cytokines.[15] In the periprosthetic osteolysis occurring in Ti-joint replacement induced by wear particles, Nrf2 has been found to be downregulated.[16] By contrast, ROS production and osteoclast differentiation, along with bone resorption, are suppressed through the Nrf2-induced nicotinamide adenine dinucleotide phosphate oxidase 4 blockade.[17] In this view, materials able to modulate the Nrf2 pathway (directly or indirectly) could be a promising approach to take.

Dental pulp stem cells (DPSCs) were previously used as a valid source for bone regeneration,[18–20] promoted by differentiation factors such as ascorbic acid (Asc), β-glycerophosphate (β-Gly), and dexamethasone (Dex), generally dissolved in the culture medium and delivered to the target cells. A limit of the canonical delivery of differentiation factors to DPSCs might be the short half-life of the dissolved factors in the growth medium, thus decreasing their effectiveness before reaching the intracellular compartment. To overcome this limitation and to better deliver necessary differentiating factors to DPSCs, the present authors have set up a cell system where a liposomal formulation (LipoMix) was tested, proving its capability to accelerate and enhance DPSC osteogenic commitment.[20]

The aim of this study was to evaluate the occurrence of DPSC osteogenic commitment cultured on Ti A by comparing the cell response obtained in the presence of conventional differentiated conditions (DM) (differentiating factors dissolved within the culture medium) with that obtained from DPSCs in the presence of the LipoMix formulation. Additionally, to investigate the modulation of inflammation in the two above mentioned experimental conditions, the expression of the master regulator of intracellular antioxidant response (the transcription factor Nrf2) and the activity of one of its enzymatic effector (catalase) were measured. Finally, Prostaglandin E2 (PGE2) secretion was evaluated to investigate whether the presence of Ti A and LipoMix might influence the release of pro-inflammatory molecules.

MATERIALS AND METHODS

Synthesis of Ti

Porous Ti specimens A (Andrew Medical) were designed and synthesized as previously described and summarized in Table 1.[7]

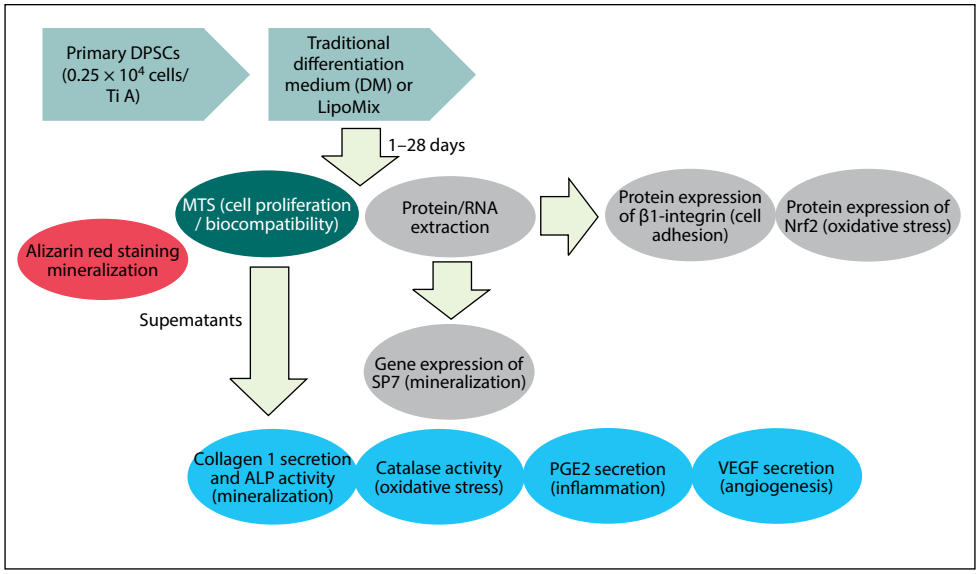

Fig 1 Schematic description of the experimental design and methods.

Preparation of Liposomes

Liposomes of POPC and/or cholesterol were prepared by using the lipid film rehydration method as described in our previous work.[20] The thin lipid film was obtained by adding 225 nmol of POPC (Avanti Polar Lipids) and 25 nmol of cholesterol (Merck) dissolved in chloroform in a round bottomed flask and drying the solution under reduced pressure at 40 °C. To embed the liposomes with hydrophilic the differentiating factors Asc and β-Gly, the phospholipid film was rehydrated for 30 min with 2 mL of phosphate buffer saline (PBS), 250 µL of Asc, and 250 µL of β-Gly. To embed the liposomes with the hydrophobic differentiating factor Dex, the liposomes were rehydrated for 30 minutes with 250 µL of Dex in DMSO mixed with 2.25 mL of PBS. Liposomes were then sonicated, sterilized, and equal volumes of the two liposomal suspensions, with the hydrophilic and hydrophobic differentiating factors, were mixed obtaining a final concentration of β-Gly, Asc, and Dex of 50 mmol/L, 1 mmol/L, and 100 nmol/L, respectively, into the final suspension. The final concentration of lipids was 0.1 mmol/L (phospholipids and cholesterol ratio= 90:10). Dimensions and surface charge (ζ-potential) of liposomes were characterized by using a dynamic laser light scattering apparatus (Brookhaven Instrument). In order to image the obtained liposomes, the Atomic Force Microscopy (AFM) analysis was performed via a MultiMode 8 AFM microscope with a Nanoscope V controller (Bruker). The sample for AFM analysis was prepared by depositing a drop of diluted suspensions of POPC-Chol liposomes on a SiO^2 wafer and then drying it in the oven at 30° Celsius for 2 hours and at room temperature overnight. The obtained sample was scanned by the silicon ScanAsyst-Air probe (triangular geometry, cantilever resonance frequency of 70 kHz, and nominal spring constant of 0.4 N/m) using ScanAsyst in Air mode. Images of 512 × 512 pixels were collected with scan sizes of 1.6 × 1.6 mm and 4 × 4 mm and were explained using the NanoScope analysis 1.8 software.

Cell Culture and Treatments

The experimental design is summarized in Fig 1.

Human DPSCs were purchased from Lonza Group, cultured up to passage 5 at 30° Celsius with 5% carbon dioxide in α-MEM medium (Merck), which was supplemented with 10% of fetal bovine serum and 1% penicillin/streptomycin (Euroclone S.p.A.). Subsequently, 0.25 × 10^4 cells were seeded on each Ti disc. The cells were allowed to adhere under culture conditions and then they were incubated with DM (Ti A + DM) or Lipo-Mix (Ti A + LipoMix) for up to 28 days. Media were replaced every 72 hours. DM condition consisted of complete α-MEM supplemented with the following osteogenic differentiating factors: Dex 10 nM, β-Gly 5 mM, and Asc 0.1 mM (Merck). LipoMix was made up of liposomes embedded with the three osteogenic differentiating factors dispersed 1:10 v/v in α-MEM, reaching in the medium at the same final concentration as the DM condition. After each experimental time point (1, 3, 7, 14, and 28 days), supernatants were collected for further analyses.

Cell Metabolic Activity (MTS Test)

Cell metabolic activity of DPSCs seeded on Ti discs and treated as previously described was measured by the 3-(4,5-dimethylthiazol-2-yl)- 5-(3-carboxymethoxyphenyl)-2-(4-sulfophenyl)-2H-tetrazolium (MTS) test. At the established time points, the assay was carried out as already reported in a previous paper by the present authors.[21]

Table 2 Primer Sequences for Quantitative PCR

Primer	Sequence (5′–3′)	Reference
18S-FW	CATGGCCGTTCTTAGTTGGT	Primer blast
18S-RW	CGCTGAGCCAGTCAGTGTAG	Primer blast
SP7-FW	CTCAGGCCACCCGTTG	Primer blast
SP7-RW	CATAGTGAACTTCCTCCTCAAGC	Primer blast

Protein Extraction and Western Blot Analysis

At the established time points, cells seeded on Ti were detached by means of trypsin and then scraped and harvested through centrifugation. Pellets were then treated as abovementioned, the supernatants were harvested, and the protein concentration was measured.[21]

A total of 15 µg of lysate for each sample were separated on a 4% to 20% SDS-PAGE Gel (ExpressPlus 10 × 8, GenScript Biotech Corporation) by electrophoresis and then underwent a transfer on a nitrocellulose membrane. The membrane was blocked in 5% non-fat milk, 10 mmol/L Tris-HCl pH 7.50, 100 mmol/L NaCl, and 0.1% (v/v) Tween-20, and then incubated at 4° Celsius and gently shook in the presence of mouse monoclonal anti-β1 Integrin (1:200), rabbit polyclonal anti-Nrf2 (1:750) (all from Santa Cruz Biotechnology), and mouse monoclonal anti-β-actin (1:5000) (Merck) primary antibodies. The day after, the membrane was probed in the presence of specific IgG horseradish peroxidase (HRP)-conjugated secondary antibodies (Calbiochem). Immunoreactive bands were revealed by means of ECL detection system (LiteAblot Extend Chemiluminescent Substrate, EuroClone), and a densitometric analysis was carried out using a ChemiDoc XRS system and the QuantiOne 1-D analysis software (BIORAD); note that densitometric values were expressed as Integrated Optical Intensity. Densitometric values were normalized on obtained values of internal β-actin.

Alizarin Red S (ARS) Staining

After 7-, 14-, and 28-days, calcium deposits indicative of cell mineralization were detected by using ARS staining. At the established time points, Ti discs were rinsed twice in PBS with $Ca2^{+}$/$Mg2^{+}$ and cell monolayer was fixed for 15 min at room temperature in paraformaldehyde 4% and then twice rinsed in distilled water. After that, each alloy was incubated with 40 mL of Alizarin Red S solution (final concentration) (Merck) at room temperature under shaking. After 20 minutes of incubation, the dye excess was removed by multiple rinses with distilled water. Calcium deposits were made soluble for the spectrophotometric evaluation by adding 800 µL/ Ti of 10% acetic acid and probed under shaking for 30 minutes. After Ti surfaces scraping, calcium deposits were collected and vortexed in a tube, followed by the addition of heated mineral oil (Merck). After 5 minutes in ice, the tubes were centrifuged at 20,000× g for 15 minutes. The Optical Density (OD) of the solution was spectrophotometrically read at 405 nm wavelength (Multiscan GO, Thermo Fisher Scientific) after the removal of the supernatant and addition of 10% ammonium hydroxide. The obtained data were normalized on RNA quantification data.

RNA Extraction

To extract RNA, a PureLink RNA Mini Kit (Life Technologies) was applied following the procedure already described.[21] The extracted RNA was eluted in 30 µL of nuclease-free water and the RNA concentration (ng/µL) was determined through Qubit RNA BR Assay Kit (Life Technologies).

Reverse Transcription and Real-Time Reverse Transcription-Polymerase Chain Reaction (Real-Time RT-PCR)

To reverse transcribe 250 ng of RNA, the high-capacity cDNA Reverse Transcription Kit (Life Technologies) was used. Reactions were carried out with volumes of 20 µL and probed in a thermal cycler following the previously described steps.[21] Gene expression was determined by quantitative PCR via the PowerUp SYBR Green Master Mix (2×) (Thermo Fisher Scientific). Each amplification reaction was carried out in a MicroAmp Optical 96-weel Reaction Plate (Life Technologies) in a final volume of 20 µL consisting of 10 µL of SYBR Green, 1 µM of each primer (stock solution 100 µM), 10 ng of cDNA, and Nuclease-Free Water. Primer sequences are reported in Table 2.

The run method consisted of the following steps: 50 ° Celsius for 2 minutes, 95 ° Celsius for 2 minutes, 40 cycles of amplification at 95 °Celsius for 15 seconds, and 60 ° Celsius for 1 minute in QuantStudio 3 (Thermo Fisher Scientific).[21] Gene expression data were then elaborated by means of QuantStudio Design and Analysis Software version 1.5.1 (Thermo Fisher Scientific). The PCR products' authenticity was confirmed by the analysis of the melt curve. The investigated gene fold changes were measured in relation to 18S ribosomal expression and it was used as housekeeping. The fold change of the SP7 gene was calculated by the comparative ΔΔCT method (relative quantification) and expressed in relation to day 1 in DM condition.

Type 1 Collagen Secretion

A human type 1 collagen enzyme-linked immunosorbent assays (ELISA) kit (Cosmo Bio) (assay limits: minimum = 0.02 µg/mL, maximum = 40 µg/mL) was used to determine the amount of collected type 1 collagen secreted in the supernatants 1, 3, 7, 14, and 28 days of culture after the procedure.[21] The absorbance of the final solution was measured at 450 nm wavelength using

a microplate reader (Multiskan GO, Thermo Scientific). The concentration of type 1 collagen (µg/mL) was calculated using a standard curve generated with specific standards provided by the kit and normalized with the amount of RNA (ng/µL) of each sample.

Alkaline Phosphatase Activity

Alkaline phosphate (ALP) activity (mU/mL/ minute) was determined through a colorimetric ALP activity assay kit (Abcam; sensitivity > 10 µU; range = 10 µU–250 µU) by using the supernatants collected at the established time points. The supernatants were pipetted in a 96-well clear flat bottom treated-culture microplate (Falcon) and incubated with 5 mmol/L pNPP substrate for 1 hour at room temperature in the dark. A stop solution was then added into each well and the absorbance was measured at 405 nm wavelength via a microplate reader (Multiskan GO, Thermo Scientific). The ALP activity was calculated following the manufacturer's instructions and normalized with the amount of RNA (ng/µL) of each sample.

Catalase Activity

The catalase activity (mU/mL) was measured after 1, 3, 7, 14, and 28 days with a colorimetric assay performed by the Amplex Red Catalase Assay kit (Molecular Probes, Thermo Fisher Scientific) while following the manufacturer's instructions. The Amplex Red reagent has greater stability, yields less background, and produces a red-fluorescent product (excitation/emission maxima ~571/585 nm) that is more readily detected than the similar reduced methylene blue derivatives commonly used for colorimetric determination of lipid peroxides in plasma, sera, cell extracts, and a variety of membrane systems.[22] The absorbance of each experimental point was measured at 560 nm wavelength and subtracted from the value of the no-catalase control. Data of the catalase activity, calculated using the standard curve, were normalized on RNA quantification data.

PGE2 Secretion

The secretion of PGE2 (pg/sample) released in the culture medium was determined through the supernatants harvested after each time point by ELISA assay (Enzo Life Sciences; range = 39.1–2,500 pg/mL; species independent) according to the manufacturer's indications. To determine the optical density values, a Multiscan GO microplate spectrophotometer (Thermo Fisher Scientific) was used, and the absorbance was read at 405 nm wavelength. The PGE2 concentration was determined by plotting the obtained values on a standard curve through the Prism5 software (GraphPad). The secretion values were normalized on RNA quantification data and expressed as means of absolute amounts of PGE2 secreted/well (pg/sample).

Table 3 Dimensions and ζ-potentials of investigated liposomes

Sample	Mean diameter (nm)	ζ-potential (mV)
Empty liposomes	371 ± 88	–6.2 ± 0.6
Liposomes + Asc + β-Gly	377 ± 70	–5.8 ± 0.7
Liposomes + Dex	313 ± 124	–10.6 ± 0.6

Vascular Endothelial Growth Factor Secretion

At the established time points (1, 3, 7, 14, and 28 days of culture), amounts (pg/mL) of human vascular endothelial growth factor (VEGF) released into the collected supernatants was read by using a VEGF ELISA kit (Enzo Life Sciences; range = 8–2,000 pg/mL; 100% cross-reactivity to human VEGF 165; no cross-reactivity to VEGF121, PDGF-AA, IL-10, GRO, Endothelin-1, big Endothelin-1, G-CSF, SCF, IL-8, HGF, or Endothelin-3.) following the manufacturer's instructions. Briefly, 100 µL of each supernatant was loaded in a well of a 96-well plate with break-apart strips coated with a mouse monoclonal antibody specific to VEGF, supplied by the kit. After 1 hour of incubation at room temperature and under gentle shaking, each well was washed with the provided wash buffer and then incubated with VEGF detector antibody for 30 minutes at room temperature. After some washes, the plate was incubated for additional 30 minutes with VEGF conjugate. A TBM solution triggered an HRP-catalyzed reaction with the generation of a blue stained solution, which turns yellow after adding a stop solution. The absorbance was read at 450 nm wavelength by a GO microplate spectrophotometer. A generated standard curve allowed the determination of VEGF pg/mL release, and it was normalized with ng/µL of RNA for each sample.

Statistics

Statistical analysis was performed by one-way ANOVA through Prism 5.0 software (GraphPad) followed by Tuckey's post-hoc test. Statistically significant values were established for $P < .05$.

Each experiment has been performed in triplicate.

RESULTS

Liposomes Characterization

The analyses performed confirmed that the embedding of hydrophilic osteogenic differentiating factors in the liposomes does not change the liposomal size (Table 3). A small reduction was observed in the case of Dex-enriched liposomes due to the fact that Dex solubilizes in the membrane bilayer thus interfering with the phospholipidic rearrangement, as previously evidenced.[18]

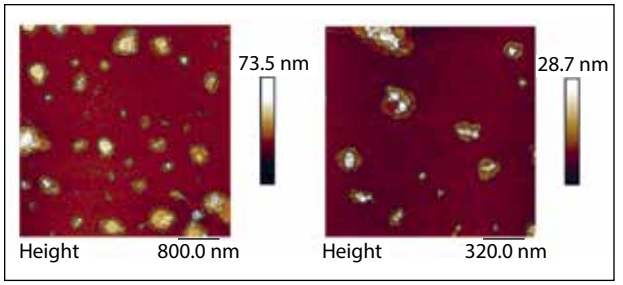

Fig 2 AFM images of representative LipoMix characterized by different magnifications. The color scale is indicative of the height of the sample.

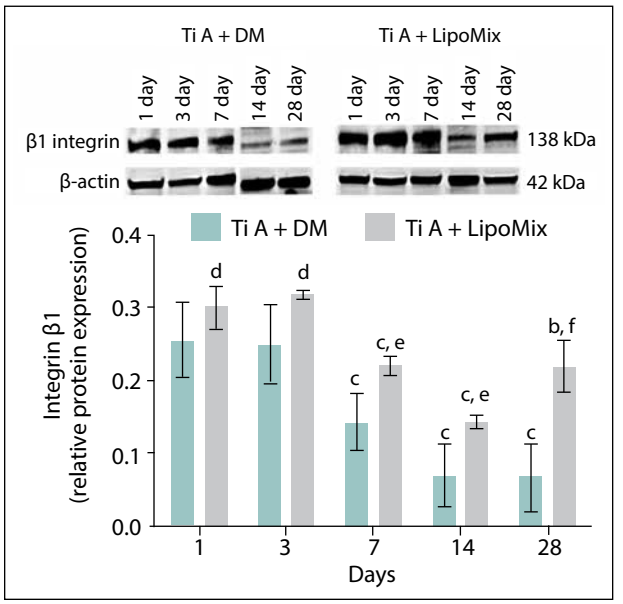

Fig 4 β1 integrin expression levels in DPSCs cultured for 1, 3, 7, 14, and 28 days in the presence of Ti A + DM or Ti A + LipoMix. The most representative of three independent western blot experiments is shown. β-actin is used as a loading control. The bar graph displays densitometric values, expressed as mean ± SD, of β1 integrin normalized on loading control. The following letters mean statistical significance: a = $P < .01$, b = $P < .001$, c = $P < .0001$ vs the same experimental condition (Ti A + DM or Ti A + LipoMix) at day 1; d = $P < .01$, e = $P < .001$, f = $P < .0001$ vs Ti A + DM at the same experimental time.

Figure 2 shows two AFM 2D height channels of diluted POPC-Chol liposomes in order to clarify the range of the representative vesicles. The color scale indicates the height of the sample and evidences the presence of flat and irregular vesicles. This feature usually represents a fixation artifact—due to the alteration induced by the drying step—leading to the formation of bilayer films spread over the surface of the SiO_2 wafer with the presence of flattened vesicles on the top of these bilayers. The dimensions of the dried liposomes are in agreement with DLS measurements. Indeed, the cross-sectional height profiles taken along different vesicles and the Particle Analysis tool in the Nanoscope software applied to the images showed that the mean diameter falls in the range of 200 ± 150 nm.

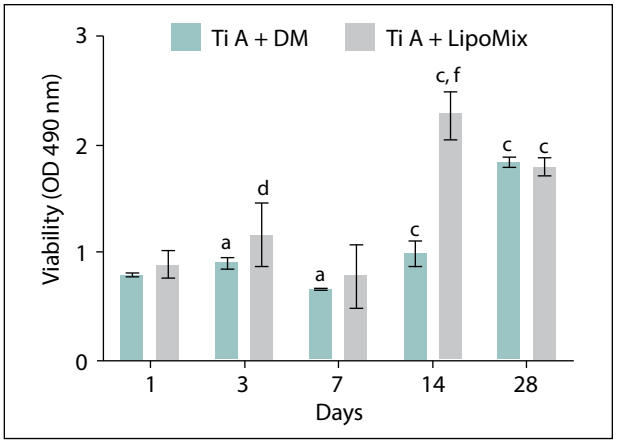

Fig 3 MTS assay performed on DPSCs cultured for 1, 3, 7, 14, and 28 days in the presence of Ti A + DM or Ti A + LipoMix. The bar graph shows the mean ± SD of three independent experiments. The following letters mean statistical significance: a = $P < .01$, b = $P < .001$, c = $P < .0001$ vs the same experimental condition (Ti A + DM or Ti A + LipoMix) at day 1; d = $P < .01$, e = $P < .001$, f = $P < .0001$ vs Ti A + DM at the same experimental time.

Cell Viability Evaluation

DPSCs seeded on Ti A were cultured in the presence of α-MEM (Ti A + DM) or LipoMix (Ti A + LipoMix) for up to 28 days. After 1, 3, 7, 14, and 28 days, cell viability was measured by the MTS test. After 3 days of culture, cells grew on Ti A + DM disclose with an appreciable increase in viability with respect to Ti A + DM at day 1; in parallel, a viability increase was recorded in cells grown on Ti A + LipoMix compared to Ti A + DM. After 7 days of culture, a statistically significant reduction of the viability rate was recorded in the Ti A + DM sample with respect to Ti A + DM at day 1. After 14 days of culture, both Ti A + DM and Ti A + LipoMix cell samples showed a significant increase compared to the same experimental conditions at day 1. In addition, cells grown in the presence of Ti A + LipoMix evidence a significant peak of viability level with respect to cells grown in the presence of Ti A + DM. Finally, after 28 days of culture, both cells grown on Ti A + DM and Ti A + LipoMix revealed an increase of viability with respect to the same experimental conditions at day 1 (Fig 3).

Evaluation of DPSC Adhesion Capability

The protein expression of β1 integrin, highly involved in the DPSC adhesion process to the surfaces, has been investigated after 1, 3, 7, 14, and 28 days of culture via a western blot analysis. In the presence of Ti A + DM, expression-levels of β1 integrin decrease in a time-dependent manner from day 1 to day 28. In parallel, cells grown on Ti A + LipoMix express β1 integrin in a higher extent compared to Ti A + DM at the same experimental times. After 7 days of culture, cells grown in the presence of Ti A + LipoMix evidence a significant

reduction of β1 integrin expression with respect to the same condition at day 1. The decrease was amplified at day 14 while after 28 days of culture, an appreciable increase in β1 integrin expression was registered (Fig 4).

Analysis of the Deposition and Mineralization of Extracellular Matrix (ECM)

In order to evaluate the deposition and mineralization process of the extracellular matrix (ECM) by DPSCs, an Alizarin red staining evidencing the calcium inorganic nodules of ECM was carried out followed by the analysis of SP7, type 1 collagen, and ALP osteogenic markers. Alizarin red staining was performed after 7 days, 14 days, and 28 days. At all tested experimental times, cells cultured in the presence of Ti A + LipoMix revealed a statistically significant increase in the matrix deposition with respect to DPSCs in the presence of Ti A + DM (Fig 5).

Then, the gene expression of the late osteogenic marker, namely SP7, was evaluated after 1, 3, 7, 14, and 28 days of culture. After 3, 7, and 28 days of culture, SP7 gene expression appears significantly reduced in cells grown both in the presence of Ti A + DM and Ti A + LipoMix with respect to the same experimental conditions at day 1. After 14 days of culture, Ti A + DM revealed a significant reduction of SP7 gene expression again compared to Ti A + DM at day 1, whereas Ti A + LipoMix showed a marked peak compared to both Ti A + LipoMix at day 1 and Ti A + DM at day 14 (Fig 6a).

Next, the secretion within the culture medium of a second well known osteogenic marker, represented by type 1 collagen, was measured by means of an ELISA assay, after 1, 3, 7, 14, and 28 days of culture. After 7 and 14 days of culture Collagen I released by DPSCs cultured on Ti A + LipoMix is significantly higher compared to both Collagen I secretion of DPSCs grown on Ti A + DM and the same experimental condition at day 1 (Fig 6b). Among the bone ECM proteins, ALP was included and thus, ALP activity was also tested after 1, 3, 7, 14, and 28 days of culture. After 1 day of culture, the recorded level of ALP activity in DPSCs cultured on Ti A+ LipoMix had statistically decreased with respect to ALP activity disclosed in the presence of Ti A+ DM. After 3, 7, and 28 days of culture, ALP activity in Ti A + DM and in Ti A + LipoMix was significantly reduced with respect to the same experimental conditions as day 1. Conversely, after 14 days of culture, a statistically significant increase in ALP activity in Ti A + LipoMix experimental condition, with respect to Ti A + DM, is disclosed in Fig 6c.

Evaluation of Oxidative Stress Counteraction

The expression of the redox-sensitive Nrf2 protein was measured through a western blot analysis after 1, 3, 7, 14, and 28 days. At the earliest experimental time (1 day), Nrf2 expression was comparable in-between the two experimental conditions. At day 3, cells weakly express Nrf2 both when cultured on Ti A + DM and on Ti + LipoMix. After 7 days of culture, the protein expression was significantly augmented in Ti A + LipoMix compared to Ti A + DM. After 14 days of culture, Nrf2 expression in Ti A + LipoMix slightly decreased compared to Nrf2 expression in the same experimental condition at day 7; however, it was higher than the ones registered for DPSCs on Ti A + DM. Finally, after 28 days, a statistically significant decrease of Nrf2 expression was recorded in Ti A + LipoMix, while levels of expression remain stable in Ti A + DM compared to day 14 (Fig 7a).

In parallel—after 1, 3, 7, 14, and 28 days of culture—the catalase activity was read finding a reduction of the enzyme activity in Ti A + LipoMix with respect to Ti A + DM after 1 and 3 days. In addition, after 3 days of culture, the enzyme activity was also significantly reduced with respect to the same experimental point at day 1. On the contrary, after 7 and 14 days of culture, catalase activity increased in the Ti A + LipoMix sample and appeared to be significantly higher with respect to the recorded values in the Ti A + DM sample. Additionally, after 7 and 28 days of culture, the recorded level was significantly reduced both in Ti A + DM and in Ti A + LipoMix compared to the same experimental conditions at day 1 (Fig 7b).

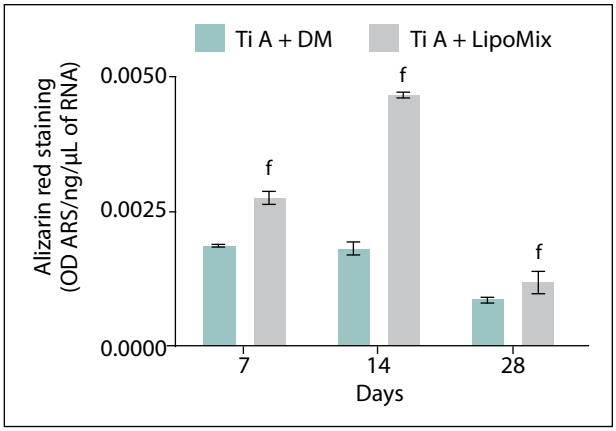

Fig 5 Alizarin red staining performed on DPSCs cultured for 7, 14, and 28 days in the presence of Ti A + DM or Ti A + LipoMix. The bar graph shows the mean ± SD of three independent experiments and represents OD values of solubilized orange-red stained calcium deposits/OD MTS ratio. The following letters mean statistical significance: a = $P < .01$, b = $P < .001$, c = $P < .0001$ vs the same experimental condition (Ti A + DM or Ti A + LipoMix) at day 1; d = $P < .01$, e = $P < .001$, f = $P < .0001$ vs Ti A + DM at day 1. OD = optical density; MTS= 3-(4,5-dimethylthiazol-2-yl)-5-(3-carboxymethoxyphenyl)2-(4-sulfophenyl)-2H-tetrazolium

Evaluation of Angiogenesis

PGE2 secretion levels were measured by means of an ELISA essay performed after 1, 3, 7, 14, and 28 days of cell culture. After 1 and 3 days of culture, the PGE2

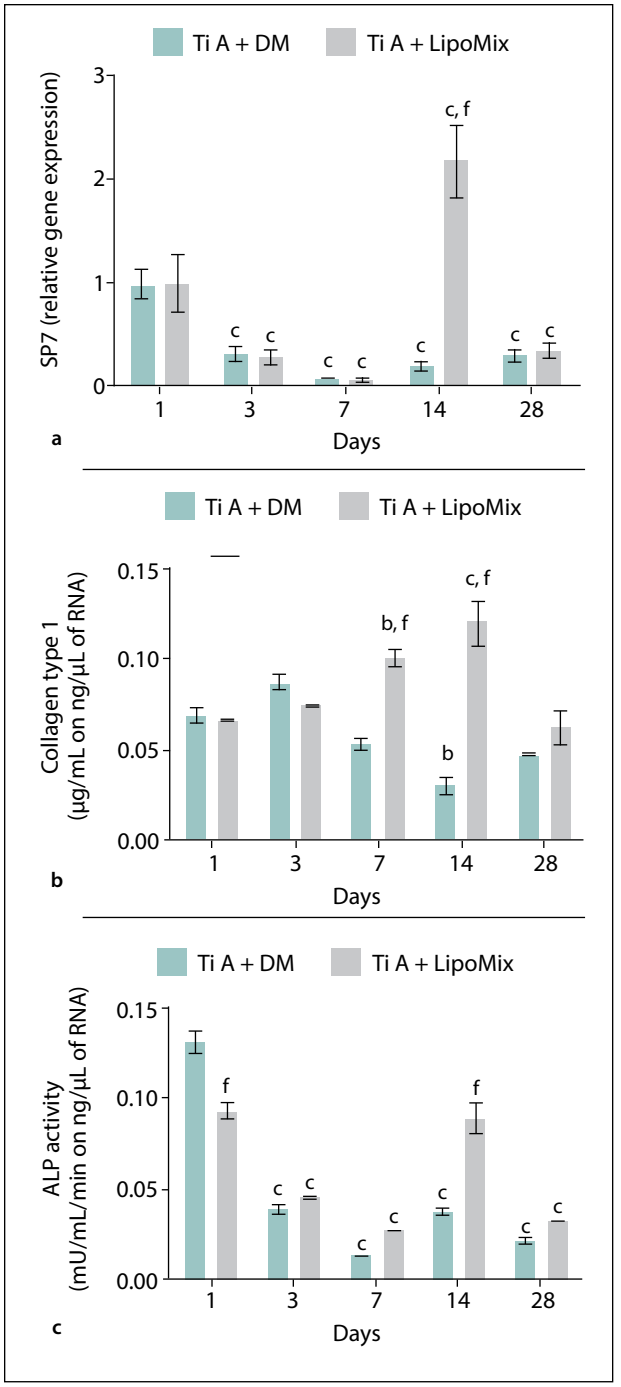

Fig 6 *(a)* Relative gene expression of SP7 in DPSCs cultured for 1, 3, 7, 14, and 28 days in the presence of Ti A + DM or Ti A + LipoMix. Data are expressed as relative to Ti A + DM at day 1 (calibrator sample defined as 1). *(b)* ELISA assay for type 1 collagen secretion in DPSCs cultured for 1, 3, 7, 14, and 28 days in the presence of Ti A + DM or Ti A + LipoMix. Secretion levels are reported as µg/mL/µL of RNA. *(c)* ALP activity in DPSCs cultured for 1, 3, 7, 14, and 28 days in the presence of Ti A + DM or Ti A + LipoMix. Bar graph showing the enzymatic activity of ALP (U/mL) were normalized on µL of RNA values. For each assay, the mean ± SD of three independent experiments is shown in all bar graphs. The following letters mean statistical significance: a = $P < .01$, b = $P < .001$, c = $P < .0001$ vs the same experimental condition (Ti A + DM or Ti A + LipoMix) at day 1; d = $P < .01$, e = $P < .001$, f = $P < .0001$ vs Ti A + DM at day 1.

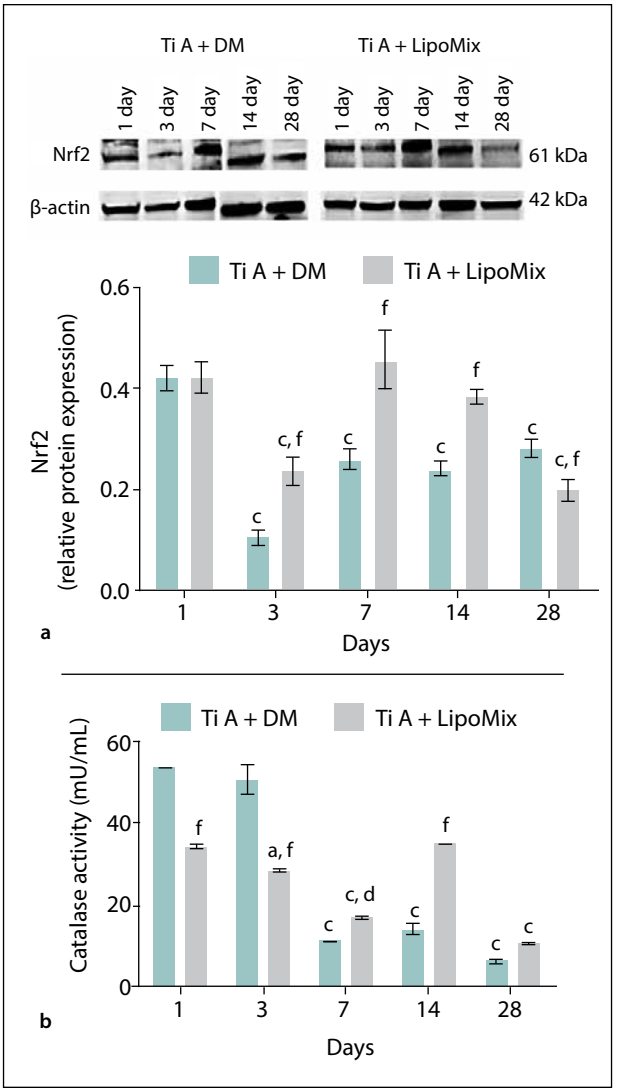

Fig 7 *(a)* Nrf2 expression levels in DPSCs cultured for 1, 3, 7, 14, and 28 days in the presence of Ti A + DM or Ti A + LipoMix. The most representative of three independent western blot experiments is shown, and β-actin is used as loading control. The bar graph displays densitometric values, expressed as mean ± SD, of Nrf2 normalized on loading control. *(b)* Catalase activity in DPSCs cultured for 1, 3, 7, 14, and 28 days in the presence of Ti + DM or Ti A + LipoMix. The bar graph shows the mean ± SD of three independent experiments and represents the activity of catalase expressed in mU/mL and normalized on RNA values. The following letters mean statistical significance: a = $P < .01$, b = $P < .001$, c = $P < .0001$ vs the same experimental condition (Ti A + DM or Ti A + LipoMix) at day 1; d = $P < .01$, e = $P < .001$, f = $P < .0001$ vs Ti A + DM at the same experimental time.

secretion of cells grown on Ti A + LipoMix were appreciably reduced compared to PGE2 levels of cells grown on Ti A + DM. Furthermore, after 3 days of culture, it was possible to evidence an increase of PGE2 level both in Ti A + DM and in Ti A+ LipoMix with respect to same experimental conditions at day 1. Conversely, after 7, 14, and 28 days of culture, a statistically significant increase in PGE2 secretion was recorded in Ti A + LipoMix with

respect to Ti A + DM. Finally, after 7, 14, and 28 days of culture, recorded PGE2 levels for Ti A + DM appeared appreciably reduced with respect to the same experimental conditions at day 1; while PGE2 measured levels in Ti A + LipoMix condition were, after 7 and 28 days, significantly reduced with respect to the same experimental condition at day 1 and, after 14 days, it significantly increased (Fig 8a).

Then, VEGF secretion was taken into consideration by measuring release levels through an ELISA assay after 1, 3, 7, 14, and 28 days of culture. At all tested experimental times, VEGF secretion levels appeared to have significantly increased in Ti A + LipoMix with respect to Ti A + DM condition. Furthermore, a statistically significant augmentation of VEGF levels was recorded after 3 and 14 days of culture in Ti A + LipoMix with respect to the same experimental condition at day 1, whereas an appreciable reduction was disclosed after 7 and 28 days with respect to the same experimental condition at day 1. Finally, VEGF release in Ti A + DM after 7, 14, and 28 days of culture had significantly increased with respect to the same experimental condition at day 1 (Fig 8b).

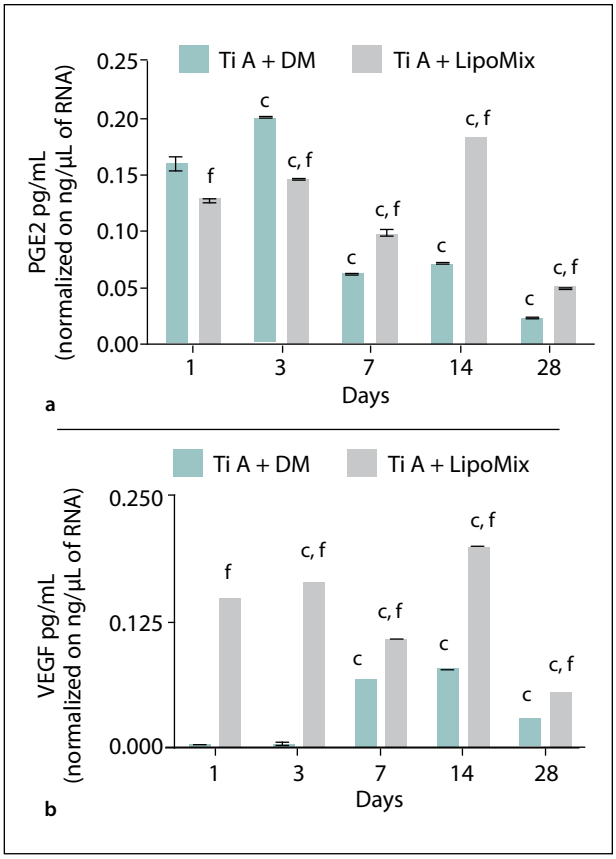

Fig 8 ELISA assay for *(a)* PGE2 and *(b)* VEGF secretion of DPSCs cultured for 1, 3, 7, 14, and 28 days in the presence of Ti A + DM or Ti A + LipoMix. Secretion levels are reported as pg/mL per RNA values (PG). The bar graph shows the mean ± SD of three independent experiments. The following letters mean statistical significance: a = $P < .01$, b = $P < .001$, c = $P < .0001$ vs the same experimental condition (Ti A + DM or Ti A + LipoMix) at day 1; d = $P < .01$, e = $P < .001$, f = $P < .0001$ vs Ti A + DM at the same experimental time.

DISCUSSION

The optimization of Ti surfaces and of their internal topography still represents a challenging goal for researchers working in regenerative dentistry. In particular, it has been previously demonstrated that a 3D-printed Ti A, with an open cell form, characterized by interconnected pores and resembling the trabecular structure of bone tissue, was able to better promote and accelerate DPSC differentiation towards the osteogenic phenotype.[7]

Standard differentiation protocols admit that mesenchymal stem cells are induced to the osteogenic phenotype when cultured in the presence of differentiating factors, such as Asc, β-Gly, and Dex; previously dissolved in the culture medium, thus reducing the effectiveness before reaching their molecular target. To guarantee an ameliorated and increased delivery of osteogenic differentiating factors directly to DPSCs, LipoMix (liposomal formulation containing differentiatin factors) was developed by our group in a previous work.[20] Thus, the current paper aimed to evaluate the efficacy of a liposome-triggered osteogenic differentiation in DPSCs cultured on an innovative 3D-printed Ti A scaffold characterized by an open cell form shape. Then, the obtained results were compared with those derived from DPSCs cultured on Ti A in the presence of DM in the standard condition.

Ti A surface architecture, in the presence of LipoMix formulation, was able to efficiently promote an appreciable DPSC viability. In particular, the open cell form of Ti A and the presence of a network of interconnected pores that were already showed in the scanning electron microscopy cross-sectional view of Ti A[7] could explain the decrease in cell viability recorded for both of the following experimental conditions: *(1)* at day 7 and *(2)* day 14. At day 7, cells that had penetrated and adhered in the deep pores of Ti A, colonized the inner structure of the alloy first—as already demonstrated in different experimental models[23]—thus, impeding to record a high viability signal at the beginning of the experimental period. The highest cell viability level was recorded later, approximately in the middle of the differentiation period at 14 days, and could be explained by admitting that cells—having filled up the inner pores network—colonized on the Ti A surface (as already disclosed in scanning electron microscopy morphologic analysis of our previous work).[7] After 14 days, a steady state could be hypothesized probably due to the achievement of a confluence state, as often found in previous reports.[18,19] Additionally, pre-osteoblasts

proliferation and attachment on 3D biomaterials are reported to be tightly regulated by the modulation of several proteins including β1 integrin (also named CD29), which is a collagen-binding protein uniformly expressed on DPSC surface[24] and time-dependently augmented during DPSC osteogenic commitment.[20] The present results were in accordance with the aforementioned studies, which underlines that the highest expression of β1 integrin indicated a pronounced capability for liposome formulation, in combination with 3D-printed Ti architecture, to promote a better and stronger cell adhesion in comparison to DM in the standard condition.

In the last few decades, ECM deposition was commonly assumed as a positive indicator of osteogenic differentiation.[25] In the present experimental model, it can be argued that the administration of differentiating factors by means of LipoMix formulation not only promoted mineralized nodules formation but also significantly anticipated their formation with respect to standard DM conditions. This hypothesis was confirmed by the expression of SP7, a transcription factor responsible (after upstream activation by RUNX2) for osteoblasts mineralization and osteoids generation.[26] This effect allows RUNX2–SP7-double-positive pre-osteoblasts differentiation into mature bone cells.[27] In accordance with this role, the presence of consistent peaks of SP7 in DPSCs exposed to liposomal formulation, confirms the early progression of the mineralization process and the efficacy of the osteogenic differentiation on the Ti A surface promoted by LipoMix. ALP is an osteogenic marker that catalyzes the hydrolysis of pyrophosphate and leads to calcium deposition, thus promoting the subsequent inorganic matrix crystals formation.[5,20] ALP enzymatic activity generally increases during stem cells osteogenic differentiation and before the beginning of matrix mineralization.[28] The ALP activity level in the present experimental model further supports the hypothesis of a positive LipoMix effect on the promotion of DPSC osteogenic differentiation. Indeed, appreciably augmented DPSC osteogenic differentiation has been found in the presence of LipoMix at day 14 with respect to DM condition. To complete the osteogenic markers panel analysis, collagen fibers—the scaffolds for the deposition of hydroxyapatite crystals[29]—were considered. Type 1 collagen secretion has been also taken into consideration finding again a peak in protein secretion in the presence of liposomal formulation. Interestingly, this information is also in accordance with β1 integrin expression and evidences a double role for this protein: *(1)* it allows cell adhesion at early times and *(2)* promotes deposition of ECM, type 1 collagen interaction, at late experimental times.

Oxidative stress is a double-edged sword because excessive amounts of oxidants cause damage to biomolecules, whereas the maintenance of a physiologic level of ROS is essential for governing crucial cell functions through redox signaling.[30] Nrf2 is the master regulator of the intracellular defense against toxic and oxidative insults because it triggers the transcription of genes involved in a oxidative stress response and ROS enzymatic detoxification, such as catalase, SOD1, and GPX.[14] Dental placement of a Ti alloy inevitably generates ROS. The process of implant placement may also lead Ti particles to enter the soft tissue and cause inflammation in gingival fibroblasts and dental pulp cells.[31] Recently, the critical role of Nrf2 in regulating antioxidant cell responses during metal implant procedures has been highlighted.[16] Analogously, the tendency during dental procedures to apply compounds capable of counteracting the excessive early oxidative stress by activating intracellular antioxidants molecular signaling is rapidly emerging.[32] Moreover, the modification of Ti roughness, implant surfaces, and their inner characteristics are crucial for determining the evolution of the cell inflammatory response in terms of cytokine secretion and anti-inflammatory signaling induction.[33] In this light, expression levels of Nrf2 were measured in our experimental model along with the activity rate of the antioxidant enzyme catalase and the pro-inflammatory mediator PGE2. DPSCs on Ti A added with LipoMix rapidly express Nrf2 and the levels of expression of Nrf2 are kept consistent for the entire experimental procedure. Despite the fact that ascorbic acid embedded in the liposome formulation was administered in minimal concentrations to trigger the secretion of collagen type 1—and thus, initiating ECM deposition to be mineralized[34]—it is plausible that it can be rapidly incorporated by cells on the Ti surface and trigger the Nrf2-mediated antioxidant response. In clinical practice, antioxidants such as ascorbic acid are choices for periodontal disease and peri-implantitis treatment, whereas oxidative stress needs to be tightly regulated at the earliest stages[32; and] thus, the administration of the innovative formulation LipoMix after the Ti application could ensure a faster absorption of antioxidants by soft tissues, which avoids compound degradation and the occurrence of lag time before the beginning of the antioxidant effect. Along the same lines, at the earliest experimental times (1 and 3 days) in the present study, catalase was activated as well but to a lesser extent with respect to Ti A + DM, whereas a switch could be detected starting from day 7 when the catalase was significantly activated by LipoMix. Finally, PGE2 levels decreased with respect to Ti A + DM at day 1 and 3 but increased after day 7, which was in agreement with the activity of catalase. It has been widely recognized that a high level of ROS is cytotoxic and inhibits normal cellular processes. However, with more recent discoveries, it is evident that ROS also plays an important and positive role in skeletal

tissue repair, specifically fracture healing.[35] In particular, the enhanced expression of catalase and its augmented activity has been demonstrated in several experimental models of osteogenesis. In addition, catalase-mimetic coatings of nanomaterials reveal a better osteoconductive profile because they protect pre-osteoblasts from oxidative stress occurrence.[36]

The process of osteoblast differentiation and bone mineralization is closely coupled to neovascularization.[37] During ossification, it is important that the condensation of the Mesenchymal stem cell signal arrives in a timely manner to the vascular cells so that osteogenic differentiation and mineralization can occur. Mesenchymal stem cells can directly signal to assist angiogenesis in fracture healing by interaction with a variety of factors (among which is VEGF). Moreover, the aggregation of mesenchymal stem cells participates in the regulation of angiogenesis by modulating redox-sensitive proteins in the endothelial compartment.[36] In the present experimental model, the VEGF secretion was strongly increased in the presence of LipoMix at all the experimental times. It was plausible to assume that the increase of the intracellular antioxidant machinery enhanced by the LipoMix contributed also to the angiogenesis promotion. Moreover, the earlier PGE2 decrease, triggered by LipoMix, is a sign of anti-inflammatory process occurrence. Similarly, the successive PGE2 increase is pro-angiogenetic being prostaglandins also involved in the promotion of neovascularization.[38] The present authors have already reported on the pro-angiogenic role of PGE2 in models of osteogenesis in the presence of DPSCs and biomaterials,[39] thus reinforcing our findings.

This study had the following limitations: *(1)* primary DPSCs should be isolated from several donors to study the heterogeneity of cell responses that are donor-related to allow authors to better identify customized Ti specimen; *(2)* rather than performing qRT-PCR on a few selected mineralization markers, it would be potentially more interesting to perform an RNAseq analysis, which could lead to the identification (potentially) of previously unknown genes involved; and *(3)* the cellular uptake of liposomes should be investigated.

To design innovative open cell forms and to customize surface properties, are crucial steps to ameliorate osseointegration and osteoconduction upon Ti-based implantation. Moreover, a balanced modulation of inflammation may represent the key event to improve soft tissue healing and osteogenic differentiation of DPSCs. In this scenario, to accelerate osteogenic cell commitment, by administering differentiating factors via innovative drug delivery systems, might further ameliorate the performance of Ti-based implants. In this light, DPSCs were here grown onto previously selected Ti A in the presence of the innovative liposomal formulation LipoMix.

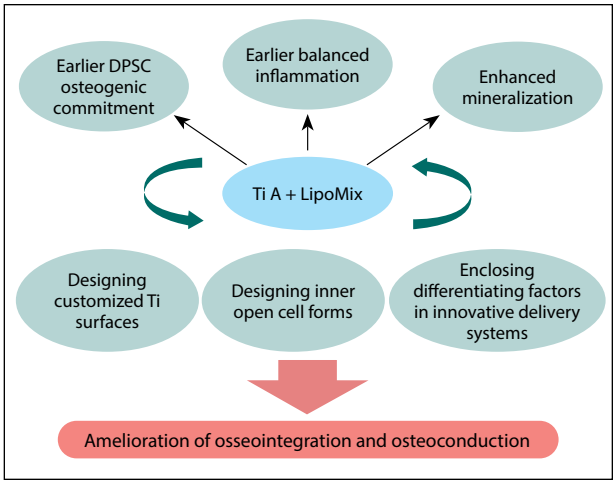

Fig 9 Schematic description of conclusions.

CONCLUSIONS

Our data confirmed the ameliorated mineralization profile of DPSC grown onto Ti A. Most important, the presence of LipoMix not only accelerated the mineralization occurrence but also led to an earlier balanced modulation of inflammation-related parameters (ie, Nrf2 expression levels and catalase activity). Results highlight that the administration of differentiating factors enclosed in an innovative delivery system and the open cell inner form of Ti A (resembling the trabecular structure of bone), were able to improve the osteogenic commitment of DPSCs and that the combination LipoMix + Ti A could represent a promising tool in regenerative dentistry. A schematic representation of the conclusions is reported in Fig 9.

However, further and deepened studies will be required to better characterize and improve the cellular uptake of liposomes to guarantee a tailored delivery of differentiating factors.

ACKNOWLEDGMENTS

This research was funded by FAR 2020, 2021 Cataldi, FAR 2020, 2021 Zara, FAR 2021 Gallorini, and by the National Operative Program (PON) Research and Innovation 2014–2020—European Social Fund, Action I. 2 "Attraction and International Mobility of Researchers" (Marialucia Gallorini). MUR National Innovation Ecosystem—Recovery and Resilience Plan (PNRR) Italy—"Innovation, digitalisation and sustainability for the diffused economy in Central Italy"- Vitality-Spoke 4 " (code ECS 00000041, CUP D73C22000840006) attributed to Prof Amelia Cataldi.

The authors deny any conflicts of interest related to this study.

Author contributions: M.G.: formal analysis, data curation, writing of original draft, and funding acquisition; A.R.: methodology, software, validation, and writing of original draft; S.P.: methodology; A.F.: resources, data curation, manuscript review and editing, and funding acquisition; C.M.: resources and visualization; A.C.: visualization, supervision, and funding acquisition; S.Z.: conceptualization, formal analysis, investigation, writing of original draft, manuscript review and editing, supervision, project administration, and funding acquisition.

REFERENCES

1. Xie Y, Li S, Zhang T, Wang C, Cai X. Titanium mesh for bone augmentation in oral implantology: Current application and progress. Int J Oral Sci 2020;12:37.
2. Jamari J, Ammarullah MI, Santoso G, Sugiharto S, Supriyono T, van der Heide E .In Silico Contact Pressure of Metal-on-Metal Total Hip Implant with Different Materials Subjected to Gait Loading. Metals 2022;12:1241.
3. Lini F, Poli PP, Beretta M, Cortinovis I, Maiorana C. Long-term retrospective observational cohort study on the survival rate of stepped screw titanium implants followed up to 20 years. Int J Oral Maxillofac Implants 2019;34:999–1006.
4. Albrektsson T, Johansson C. Osteoinduction, osteoconduction and osseointegration. Eur Spine J 2001;10(suppl 2):S96–S101.
5. Hou C, Liu Y, Xu W, et al. Additive manufacturing of functionally graded porous titanium scaffolds for dental applications. Biomater Adv 2022;139:213018.
6. Mangano F, Chambrone L, van Noort R, Miller C, Hatton P, Mangano C. Direct metal laser sintering titanium dental implants: A review of the current literature. Int J Biomater 2014;2014:461534.
7. Gallorini M, Zara S, Ricci A, Mangano FG, Cataldi A, Mangano C. The open cell Form of 3D-printed titanium improves osteconductive properties and adhesion behavior of dental pulp stem cells. Materials (Basel) 2021;14:5308.
8. Baseri M, Radmand F, Hamedi R, Yousefi M, Kafil HS. Immunological aspects of dental implant rejection. Biomed Res Int 2020;2020,7279509.
9. Mavrogenis AF, Dimitriou R, Parvizi J, Babis GC. Biology of implant osseointegration. J. Musculoskelet. Neuronal Interact 2009;9:61–71.
10. Zhao Z, Zhao Q, Gu B, et al. Minimally invasive implantation and decreased inflammation reduce osteoinduction of biomaterial. Theranostics 2020;10:3533–3545.
11. Franz S, Rammelt S, Scharnweber D, Simon JC. Immune responses to implants - A review of the implications for the design of immunomodulatory biomaterials. Biomaterials 2011;32:6692–6709.
12. Abaricia JO, Shah AH, Musselman RM, Olivares-Navarrete R. Hydrophilic titanium surfaces reduce neutrophil inflammatory response and NETosis. Biomater Sci 2020;21:2289–2299.
13. Kobayashi EH, Suzuki T, Funayama R, et al. Nrf2 suppresses macrophage inflammatory response by blocking proinflammatory cytokine transcription. Nat Commun 2016;7:11624.
14. He F, Ru X, Wen T. NRF2, a transcription factor for stress response and beyond. Int J Mol Sci 2020;21:4777.
15. Ma F, Luo S, Lu C, et al. The role of Nrf2 in periodontal disease by regulating lipid peroxidation, inflammation and apoptosis. Front Endocrinol (Lausanne) 2022;13:963451.
16. Dong J, Zhang L, Ruan B, et al. NRF2 is a critical regulator and therapeutic target of metal implant particle-incurred bone damage. Biomaterials 2022;288:121742.
17. Wang W, Liang X, Liu X, et al. NOX4 blockade suppresses titanium nanoparticle-induced bone destruction via activation of the Nrf2 signaling pathway. J Nanobiotechnology 2022;20:241.
18. De Colli M, Radunovic M, Zizzari VL, et al. Osteoblastic differentiating potential of dental pulp stem cells in vitro cultured on a chemically modified microrough titanium surface. Dent Mater J 2018;37:197–205.
19. Di Carlo R, Di Crescenzo A, Pilato S, et al. Osteoblastic differentiation on graphene oxide-functionalized titanium surfaces: An in vitro study. Nanomaterials (Basel) 2020;10:654.
20. Gallorini M, Di Carlo R, Pilato S, et al. Liposomes embedded with differentiating factors as a new strategy for enhancing DPSC osteogenic commitment. Eur Cell Mater 2021;41:108–120.
21. Ricci A, Gallorini M, Feghali N, Sampò S, Cataldi A, Zara S. Snail slime extracted by a cruelty free method preserves viability and controls inflammation occurrence: A focus on fibroblasts. Molecules 2023;28:1222.
22. Karakuzu O, Cruz MR, Liu Y, Garsin DA. Amplex red assay for measuring hydrogen peroxide production from caenorhabditis elegans. Bio Protoc 2019;9:e3409.
23. Liu Z, Xu Z, Wang X, et al. Construction and osteogenic effects of 3D-printed porous titanium alloy loaded with VEGF/BMP-2 shell-core microspheres in a sustained-release system. Front Bioeng Biotechnol 2022;10:1028278.
24. Gronthos S, Arthur A, Bartold PM, Shi S. A method to isolate and culture expand human dental pulp stem cells. Methods Mol Biol 2011;698:107–121.
25. Li X, Zheng Y, Zheng Y, et al. Circular RNA CDR1 as regulates osteoblastic differentiation of periodontal ligament stem cells via the miR-7/GDF5/SMAD and p38 MAPK signaling pathway. Stem Cell Res Ther 2018;9:232.
26. Nakashima K, Zhou X, Kunkel G, et al. The novel zinc fin-ger-containing transcription factor osterix is required for osteoblast differentiation and bone formation. Cell 2002;108:17–29.
27. Maes C, Kobayashi T, Selig MK, et al. Oeoblast precur-sors, but not mature osteoblasts, move into developing and fractured bones along with invading blood vessels. Dev Cell 2010;19:329–344.
28. Wu X, Stroll SI, Lantigua D, Suvarnapathaki S, Camci-Unal G. Eggshell particle-reinforced hydrogels for bone tissue engineering: An orthogonal approach. Biomater Sci 2019;7:2675–2685.
29. Franceschi RT, Xiao G, Jiang D, Gopalakrishnan R, Yang S, Reith E. Multiple signaling pathways converge on the Cbfa1/Runx2 transcription factor to regulate osteoblast differentiation. Connect Tissue Res 2003;44(suppl 1):S109–S116.
30. Sies H, Berndt C, Jones DP. Oxidative stress. Annu Rev Biochem 2017;86:715–748.
31. Bressan E, Ferroni L, Gardin C, et al. Metal nanoparticles released from dental implant surfaces: Potential contribution to chronic inflammation and peri-implant bone loss. Materials 2019;12:2036.
32. Qi F, Huang H, Wang M, Rong W, Wang J. Applications of antioxidants in dental procedures. Antioxidants (Basel) 2022;11:2492.
33. Karcı B, Öncü E, Dogan M. The effect of different dental implant surface characteristics on bone immunologic biomarkers and microbiologic parameters: A randomized clinical study. Int J Periodontics Restorative Dent 2021;41:589–597.
34. Langenbach F, Handschel J. Effects of dexamethasone, ascorbic acid and β-glycerophosphate on the osteogenic differentiation of stem cells in vitro. Stem Cell Res Ther 2013;4:117.
35. Sheppard AJ, Barfield AM, Barton S, Dong Y. Understanding reactive oxygen species in bone regeneration: A glance at potential therapeutics and bioengineering applications. Front Bioeng Biotechnol 2022;10:836764.
36. Liu S, Li K, Hu T, et al. X. Zn-doped MnO2 nanocoating with enhanced catalase-mimetic activity and cytocompatibility protects pre-osteoblasts against H2O2-induced oxidative stress. Colloids Surf B Biointerfaces 2021;202:111666.
37. Percival CJ, Richtsmeier JT. Angiogenesis and intramembranous osteogenesis. Dev Dyn 2013;242:909–922.
38. Namkoong S, Lee SJ, Kim CK, et al. Prostaglandin E2 stimulates angiogenesis by activating the nitric oxide/cGMP pathway in human umbilical vein endothelial cells. Exp Mol Med 2005;37:588–600.
39. Rapino M, Di Valerio V, Zara S, et al. Chitlac-coated thermosets enhance osteogenesis and angiogenesis in a Co-culture of dental pulp stem cells and endothelial cells. Nanomaterials (Basel) 2019;9:928.